TRANSACTIONS OF THE INSTITUTE OF AVIATION ISSN 2300-5408
No. 4 (237), pp. 63-75, Warsaw 2014

EXPERIMENTAL RESEARCH OF TANDEM-SCHEME UAV MODEL AERODYNAMIC CHARACTERISTICS

OLEXANDR M. MASKO*, ILLIA S. KRYVOKHATKO**, PROF. VITALIY V. SUKHOV***

** Experimental Design Office of General Aviation, Petropavlivska Borschagivka, „Chayka" urochishche, Kyevo-Svyatoshyn distr., Kyiv reg., Ukraine*

***Antonov Aeronautical Scientific-Technical Complex, 1, Akademika Tupoleva str., Kyiv, Ukraine*

****Faculty of Aviation and Space Systems, National Technical University of Ukraine "Kyiv Polytechnic Institute", Peremogy av., 37, build. 28, Kyiv, Ukraine*

maska310@ukr.net, elijah@ukr.net, suhovkpi@gmail.com

Abstract

Tandem-wing aerodynamic scheme became widespread for tube launch UAV due to possibility of required flight performance realization under tight dimension constraints. In this work results of wind tunnel weight and visual tests of UAV model with wingspans about 1 m are presented. Model aerodynamic characteristics were defined by six-component wind tunnel balance at Mach number 0.075 and Reynolds number 187 000 calculated for one wing chord of 0.11 m. Model stagger (390, 490, 590 mm), rear wing dihedral angle (0°, -5°, -9°), forward-to-rear wingspan ratio (0.67; 0.9; 0.92; 1.24) were variable. It was determined that model is longitudinal and directional static stable, has high maximal lift-drag ratio (in range from 10.6 to 13.7) and acceptable maximal lift coefficient without flaps (from 1.05 to 1.09) and critical angle of attack (from 15.1 to 16.4°). Stagger increasing leads to zero or positive maximal lift-drag ratio increasing. If forward wing span is larger than rear wing span than stagger increasing is more effective with zero dihedral angle. If rear wing span is larger than forward wing span than stagger increasing is more effective with negative dihedral angle.

Keywords: UAV, tandem-scheme, aerodynamic characteristics, wingspan, stagger, dihedral angle.

INTRODUCTION

The most widespread class of unmanned aerial vehicle (UAV) is Man Portable (transport mass less than 10…15 kg [1]) which includes micro-UAV (with flight mass under 5 kg [2]). Rational development of this class UAV is tube launch UAV which is starting from container that means tight dimension constraints including wingspan limitation. Tandem scheme became popular among such UAV due to sufficient wingspan decreasing because of wing area dividing into two surfaces [3]. Though many questions about tandem scheme aerodynamic characteristics remain without answer, for example, aerodynamic configuration, payload arrangement, analytical methods of aerodynamic characteristics definition.

PROBLEM STATEMENT

The purpose of this study is to define tandem scheme model aerodynamic characteristics and to research an influence of stagger (longitudinal distance between leading edges of two wings) on model aerodynamic characteristics. Dihedral angle effect was considered in previous article [4].

EXPERIMENT CONDITIONS

Chords of both wings equaled to 110 mm; airfoil MH32 of 12 % relative thickness and without geometric twist was used (fig. 1). Forward high-wing was fixed at an angle of setting equaled to -4.2° to fuselage waterline (FWL) and dihedral angle equaled to -4°.

Rear low-wing was set in one of three longitudinal positions (stagger: x_1, x_2, x_3) and for each position one of three dihedral angle was set ψ = 0°; ψ = -5° и ψ = -9°. Rear wing angle of setting was 0°.

Wingspans were variable from 1050 mm to 1450 mm for forward wing and from 1170 to 1570 mm for rear wing due to side inserts of 95 mm chord and 8.7 % relative thickness (fig. 2; tab. 1).

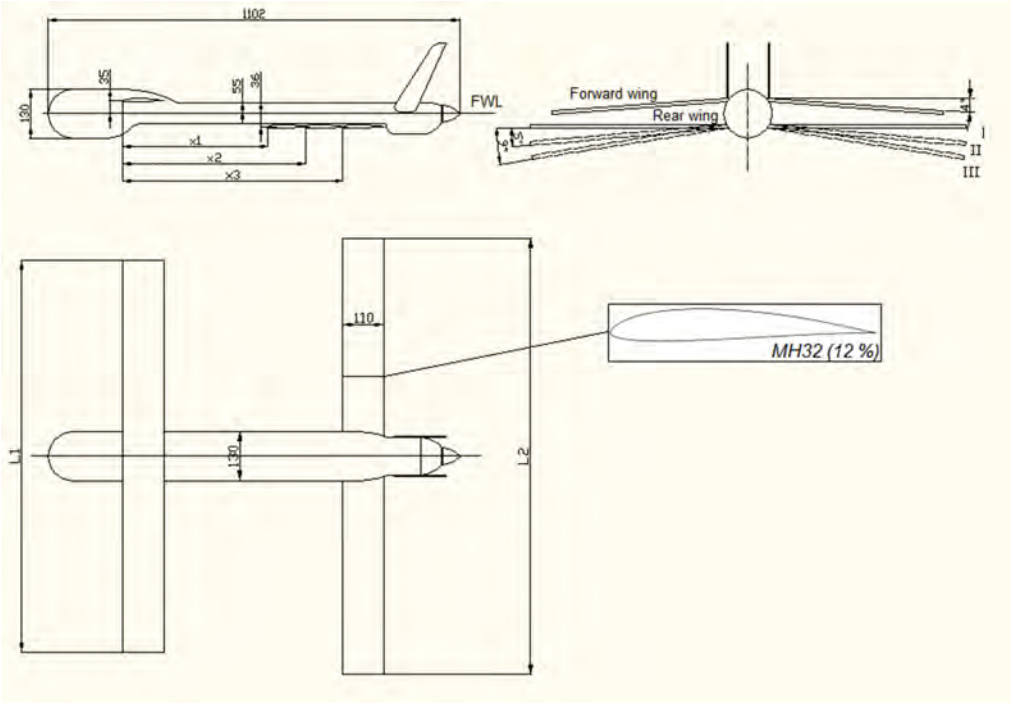

Fig. 1. Model geometry [Kryvokhatko-Masko-Sukhov, 2012]

It should be noticed that real tandem-scheme air vehicles has angle of forward wing setting higher than rear wing one for longitudinal stability providing in wide angle-of-attack range [5]. Testing model was performed with higher angle of rear wing setting for aerodynamic between-wing interference research. Also at cruise angle of attack stagger increasing from to leads to between-wing height increasing equaled to 21 mm. So in experiment we are not able to separate two geometrical parameters effect completely.

Fig. 2. Model in the wind tunnel [Kryvokhatko-Masko-Sukhov, 2013]

Tab. 1. Model geometry variables [Kryvokhatko-Masko-Sukhov, 2012]

Configuration	Configuration parameters									
	Wingspan, mm	Stagger x, mm								
		x_1 = 390			x_2 = 490			x_3 = 590		
		Rear wing dihedral angle ψ,°								
		0	-5	-9	0	-5	-9	0	-5	-9
1–1	L_1 = 1050 L_2 = 1170	+	+	+	+	+	+	+	+	+
1–2	L_1 = 1050 L_2 = 1570	+	+	+	+	+	–	+	+	+
2–1	L_1 = 1450 L_2 = 1170	+	+	+	–	–	–	+	+	+
2–2	L_1 = 1450 L_2 = 1570	+	–	+	–	–	–	+	–	+

Model aerodynamic performance was defined by six-component balance in certified wind tunnel AT-1 at flow velocity of V = 25 *m/s* that corresponds to Mach number of M = 0.075 and Reynolds number of Re = 1.87 x 10^5 calculated for one wing chord.

RESULTS

Effect of stagger on aerodynamic characteristics research

Results of stagger effect research are presented graphically on fig. 3÷15.
For configuration 1–1 tests of model with and without fin were performed (fig. 3÷7).

Stagger increasing from x_3 = 390 *mm* to x_3 = 590 *mm* results in maximal lift-drag ratio growth, maximal lift coefficient decreasing, and upward shift of C_L (α) dependency in linear range:
– for : ψ = 0°: $\Delta (L/D)_{max} \approx 0.23$ (with fin); $\Delta C_{Lmax} \approx -0.03$, $\Delta C_L \approx +0.04$;
– for : ψ = -5°: $\Delta (L/D)_{max} \approx 0.4$ (with/without fin), $\Delta C_L \approx +0.075$;
– for : ψ = -9°: $\Delta (L/D)_{max} \approx 0.6$ (with fin) and $\Delta (L/D)_{max} \approx 0.7$ (without fin); C_{Lmax} increases; $\Delta C_L \approx +0.015$.

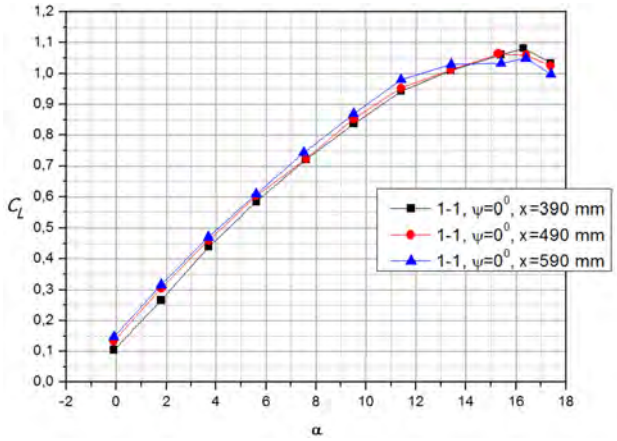

Fig. 3. Lift coefficient graph [Kryvokhatko-Masko-Sukhov, 2013]

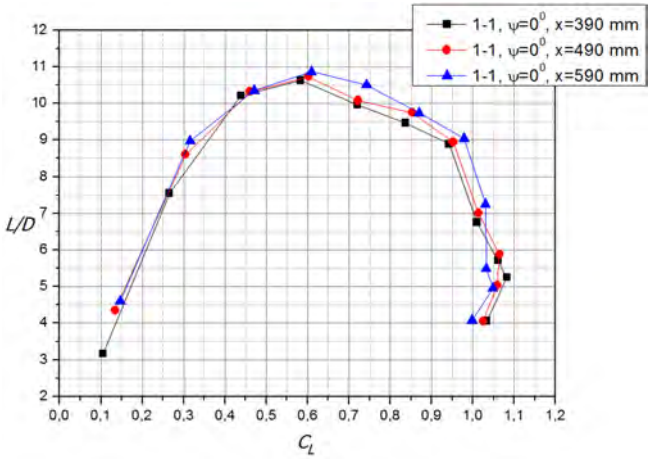

Fig. 4. Lift-drag ratio graph [Kryvokhatko-Masko-Sukhov, 2013]

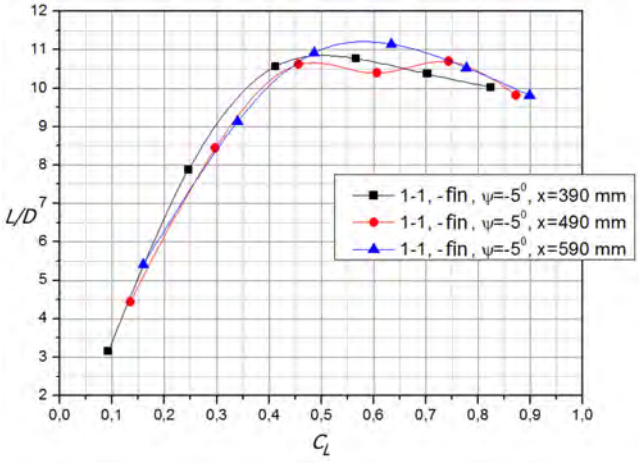

Fig. 5. Lift-drag ratio graph [Kryvokhatko-Masko-Sukhov, 2013]

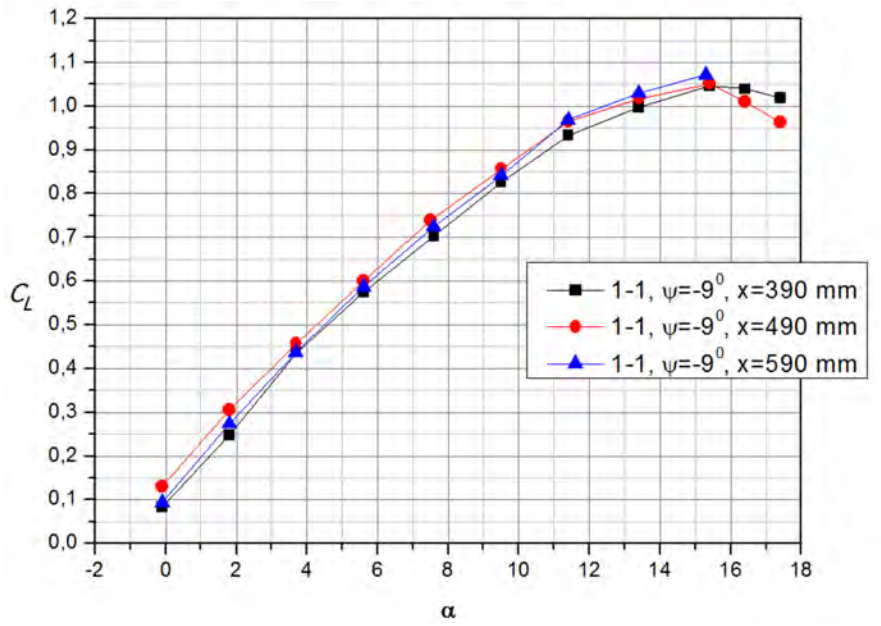

Fig. 6. Lift coefficient graph [Kryvokhatko-Masko-Sukhov, 2013]

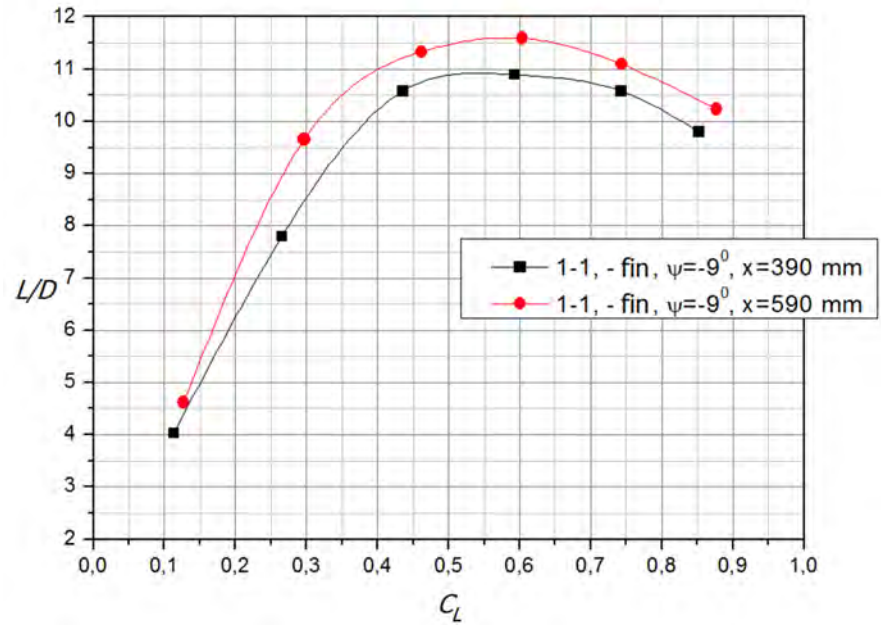

Fig. 7. Lift-drag ratio graph [Kryvokhatko-Masko-Sukhov, 2013]

For configuration 2–2 stagger increasing from $x_3 = 390mm$ to $x_3 = 590mm$ results in maximal lift-drag ratio increasing and maximal lift coefficient decreasing (fig. 8, 9):
– for : $\psi = 0°$: $\Delta (L/D)_{max} \approx 0.0$ (within the experimental error) and $\Delta C_{Lmax} \approx -0.01$;
– for : $\psi = -9°$: $\Delta (L/D)_{max} \approx 1.05$ and $\Delta C_{Lmax} \approx -0.02$.

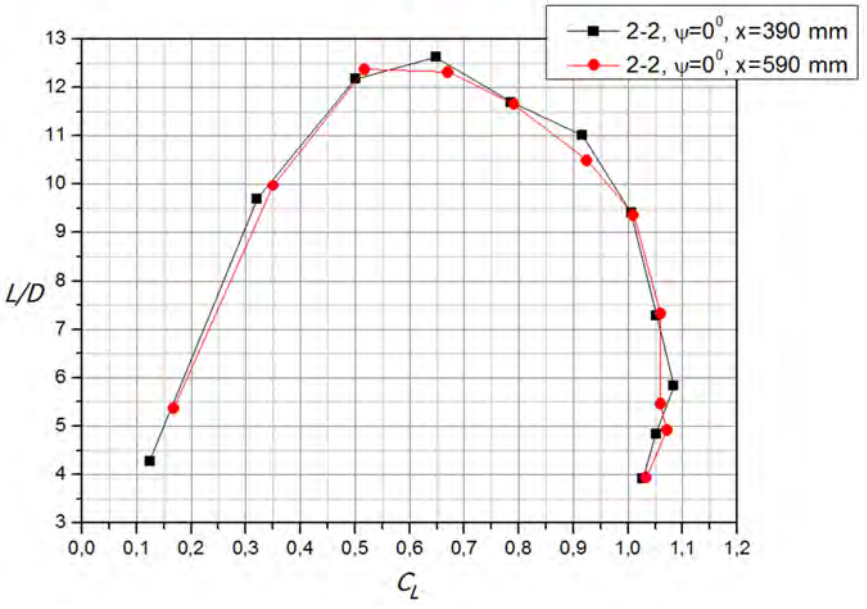

Fig. 8. Lift-drag ratio graph [Kryvokhatko-Masko-Sukhov, 2013]

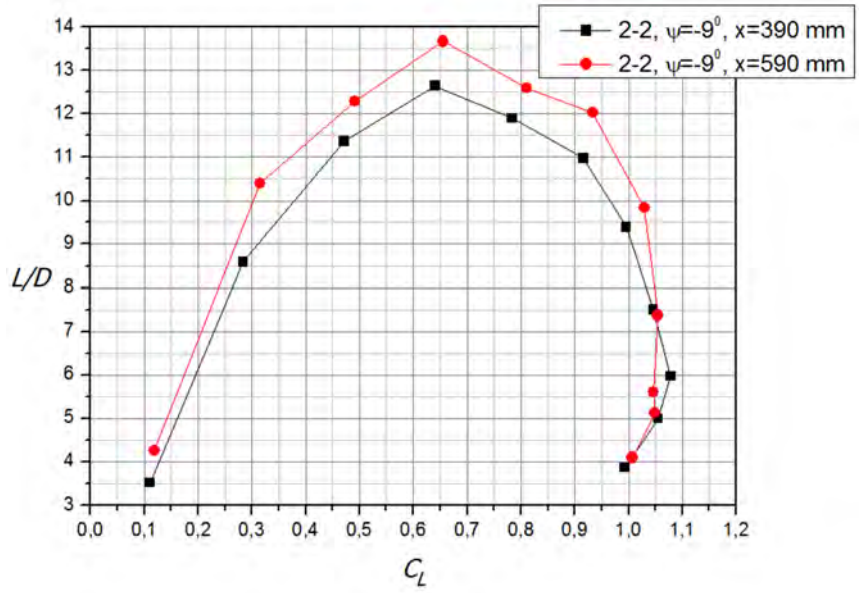

Fig. 9. Lift-drag ratio graph [Kryvokhatko-Masko-Sukhov, 2013]

For configuration 1–2 tests of model without fin were performed. Stagger increasing from $x_3 = 390mm$ to $x_3 = 590mm$ results in upward shift of graph $C_L(\alpha)$ (as for configuration 1–1) and maximal lift-drag ratio growth (fig. 10, 11):
– for $\psi = 0°$: $\Delta (L/D)_{max} \approx 0.00$; $\Delta C_{Lmax} \approx +0.03$;
– for $\psi = -5°$: $\Delta (L/D)_{max} \approx 0.6$; $\Delta C_{Lmax} \approx +0.07$;
– for $\psi = -9°$: $\Delta (L/D)_{max} \approx 1.15$; $\Delta C_{Lmax} \approx +0.025$.

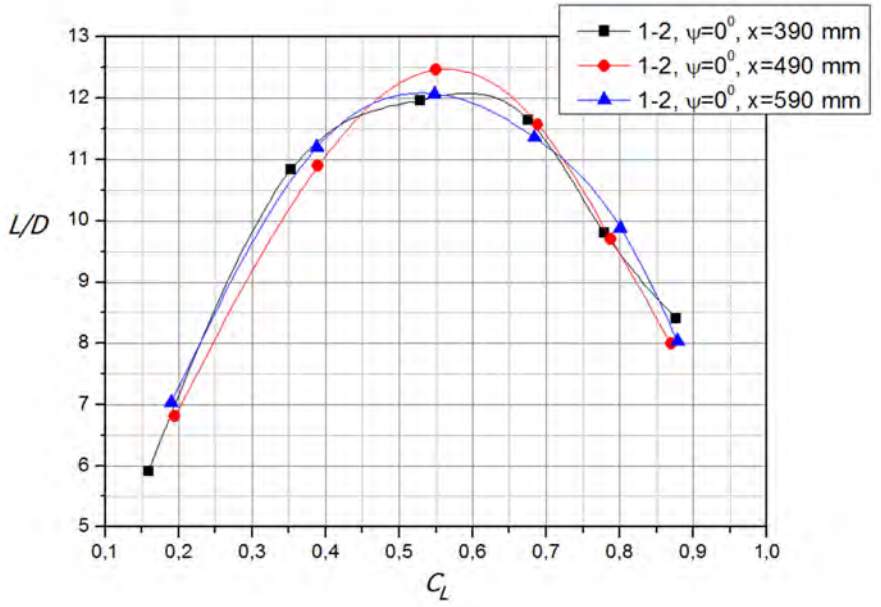

Fig. 10. Lift-drag ratio graph [Kryvokhatko-Masko-Sukhov, 2013]

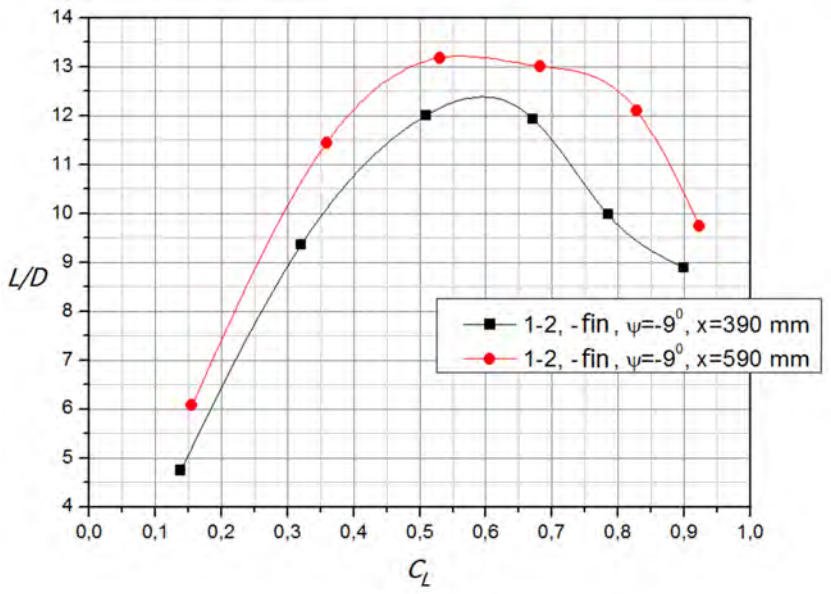

Fig. 11. Lift-drag ratio graph [Kryvokhatko-Masko-Sukhov, 2013]

For configuration 2–1 tests of model with fin were performed. Stagger increasing from x_3 = 390*mm* to x_3 = 590*mm* results in upward shift of graph $C_L(\alpha)$ in linear range, maximal lift-drag ratio and maximal lift coefficient changing (fig. 12÷15):

– for $\psi = 0°$: $\Delta (L/D)_{max} \approx 1.15$; $\Delta C_{Lmax} \approx -0.01$, $\Delta C_L \approx +0.03$;

– for $\psi = -5°$: $\Delta (L/D)_{max} \approx 0.0$; $\Delta C_{Lmax} \approx 0.00$, $\Delta C_L \approx +0.045$;

– for $\psi = -9°$: $\Delta (L/D)_{max} \approx 0.0$; $\Delta C_{Lmax} \approx +0.01$, $\Delta C_L \approx +0.00$.

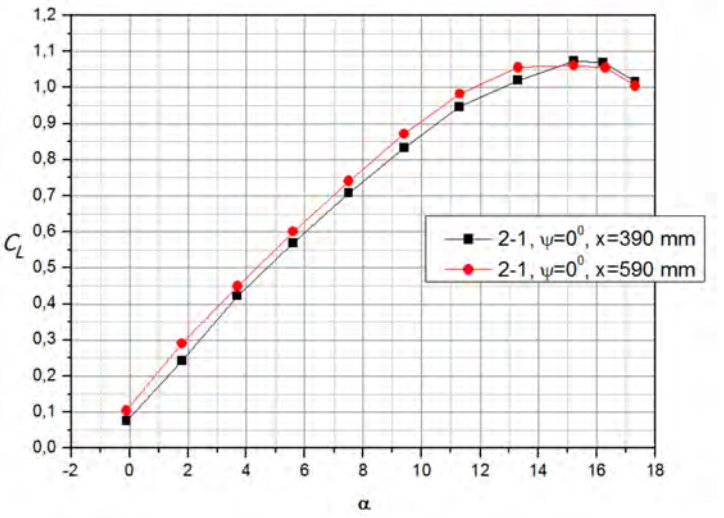

Fig. 12. Lift coefficient graph [Kryvokhatko-Masko-Sukhov, 2013]

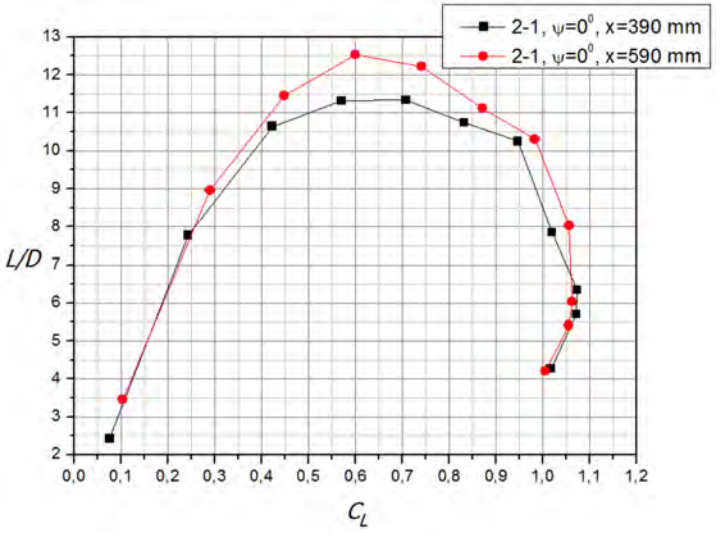

Fig. 13. Lift-drag ratio graph [Kryvokhatko-Masko-Sukhov, 2013]

It can be seen that for configuration 2-1 maximal lift-drag ratio increasing due to stagger increasing is higher if $\psi = 0°$. In contrast to it for other configurations (1-1, 1-2, 2-2) stagger increasing is more effective for lift-drag ratio gain if $\psi = -9°$. So for configuration 2-1 derivative $\frac{\partial (L/D)_{max}}{\partial x}$ is maximal if $\psi = 0°$, and for the others – if $\psi = -9°$.

Effect of stagger on maximal lift-drag ratio for configuration 1-1 is presented on fig. 16.

Basic model aerodynamic characteristics

For basic model (configuration 1-1, $\psi = 0°$, x_3=590mm) following aerodynamic characteristics have been achieved:

- maximal lift-drag ratio: $(L/D)_{\max} = (L/D)_{CL=0.6} = 10.85$;
- maximal lift coefficient: $C_{L\max} = 1.05$ at $\alpha_{stall} = 16.4°$;
- lift slope: $C_L^{\alpha} = 0.072 \frac{1}{°}$; lift coefficient at zero angle of attack: $C_{L0} = 0.15$;
- minimal drag coefficient: $C_{D\min} = 0.032$;
- static longitudinal stability degree: $m_z^{CL} = -0.14$;
- static rolling stability degree at α = 6.6°: $m_x^{\beta} = -0.0010 \frac{1}{°}$;
- static directional stability degree at α = 6.6°: $m_y^{\beta} = -0.0021 \frac{1}{°}$.

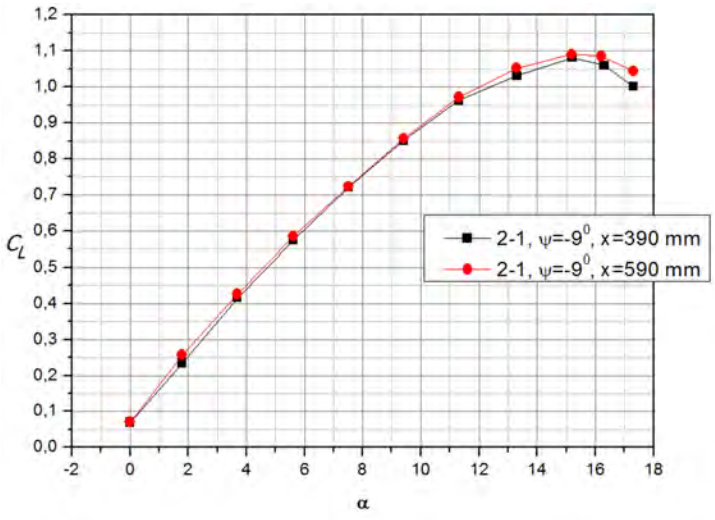

Fig. 14. Lift coefficient graph [Kryvokhatko-Masko-Sukhov, 2013]

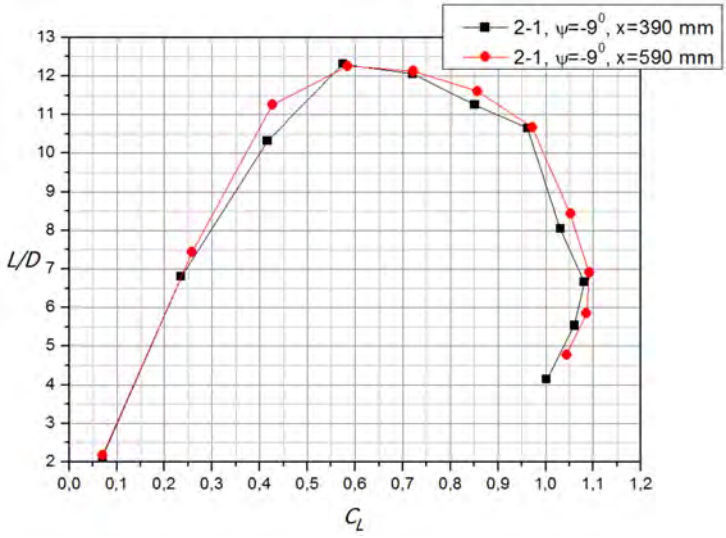

Fig. 15. Lift-drag ratio graph [Kryvokhatko-Masko-Sukhov, 2013]

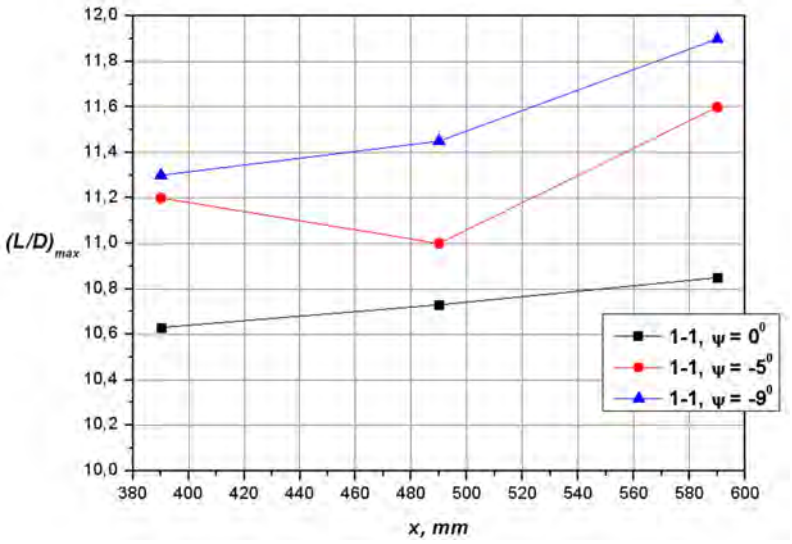

Fig. 16. Maximal lift-drag ratio graph [Kryvokhatko-Masko-Sukhov, 2013]

ANALYSIS

Maximal lift-drag ratio of normal-scheme tube launch UAV at comparable Reynolds number equals to 9 [6]. So tandem-scheme UAV model obtained high maximal lift-drag ratio for tube launch UAV.

It`s known that if distance between tip vortices grows up then total induced drag is decreasing and maximal lift-drag ratio is increasing [7]. It was found experimentally that stagger increasing results in zero or positive gaining of maximal lift-drag ratio depending of wingspans ratio and dihedral angle. Newly founded dependencies are:

- if forward wingspan is larger than rear wingspan (wingspans ratio higher than 1) maximal lift-drag ratio increasing due to stagger increasing is higher for zero lower wing dihedral angle;
- if rear wingspan is larger than forward wingspan (wingspans ratio lower than 1) stagger increasing is more effective for lift-drag ratio increasing for negative lower wing dihedral angle.

Symmetry of vortex system proved that dependencies concerned to negative lower wing dihedral angle are the same for positive upper wing dihedral angle.

It was mentioned above that stagger increasing (from 390 mm to 590 mm) results in between-wing height increasing (21 mm). Nevertheless founded dependencies reason is horizontal position of tip vortices. Configurations 1–1 and 2–1 have the same between-wing height for the same stagger, but different wingspans ratios indeed. So the dependencies of dihedral angle effect on lift-drag ratio are opposite for these configurations because vortices pushes each other opposite too: forward wing vortex is pushed inside and rear wing vortex – outside for configuration 1–1; forward wing vortex is pushed outside and rear wing vortex – inside for configuration 2–1. Monoplane tip vortex visualization is shown on fig. 17, tandem tip vortices repulsion visualization – on fig. 18–19.

For theoretical explanation of found dependencies the hypothesis of Π-form vortices is helpless. According to Munk theorems [8] stagger has no influence on tandem-scheme aerodynamic performance and there is no explanation to experimental results.

CONCLUSIONS

In present research experimentally found tandem-scheme UAV model aerodynamic characteristics and stagger effect on these characteristics were analyzed.

UAV model demonstrated high maximal lift-drag ratio, acceptable maximal lift coefficient and angle-of-attack range that proves the topicality of tandem-wing aerodynamic scheme for tube launch UAV.

The dependencies of wing dihedral angle on stagger derivative of lift-drag ratio were found that can`t be explained with help of classical biplane theory.

Visual tests for different model geometric parameters proof complex form of the vortex system (vortices are far from theoretical Π-liked ones) because of intensive vortices interaction (repulsion of unidirectional and attraction of oppositely directed vortices) that results in rear wing circulation redistribution and air vehicle induced drag changing. This interaction should be taken into account for real tandem-scheme UAV/aircraft aerodynamic characteristics definition.

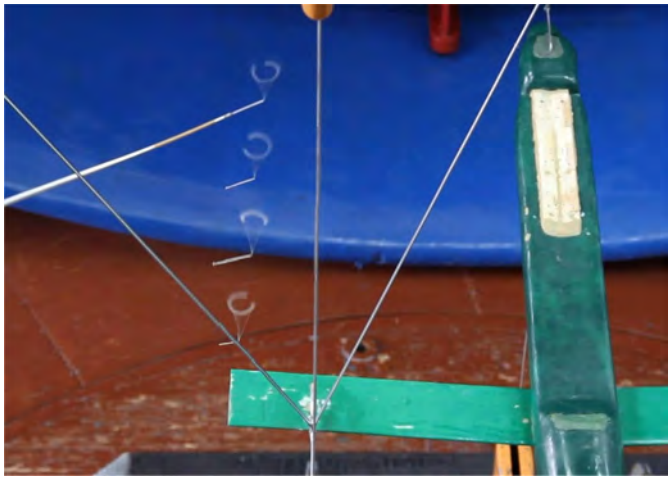

Fig. 17. Monoplane vortex visualization (configuration 1–0) [Kryvokhatko-Masko-Sukhov, 2013]

Fig. 18. Tandem-wing vortices visualization (configuration 1–1, $\psi = 0°$, x_3=490mm) [Kryvokhatko-Masko-Sukhov, 2013]

So the ways to increase tandem-scheme UAV/aircraft maximal lift-drag ratio are:
- optimal wingspans ratio precise defining;
- wingspans increasing at constant wingspan ratio;
- between-wing height and stagger increasing;
- dihedral wing angle exploiting: positive for high-wing and negative for low-wing.

Dimensions constraints for tube launch UAV results in wingspans limitations before start so it`s logical to consider telescopic wing application to increase wingspans during flight [9, 10]. Experimental results of lift coefficient and lift-drag ratio values are correct for given geometry and Reynolds number. Discovered dependencies of stagger effect on aerodynamic characteristics can be used for tandem-scheme UAV/aircraft design for low Mach number.

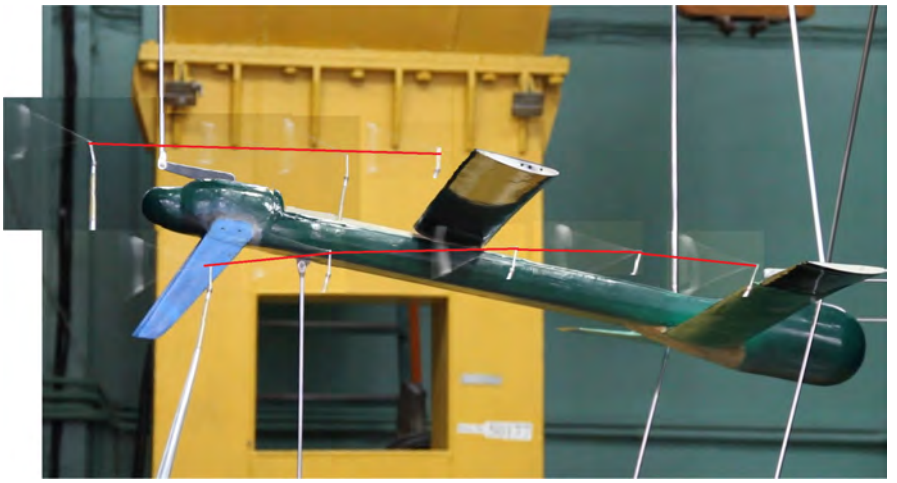

Fig. 19. Tandem-wing vortices visualization (configuration 2–1, $\psi = 0°$, x_3=390mm) [Kryvokhatko-Masko-Sukhov, 2013]

LITERATURE

[1] Danyk Yu. H. (2008). Bezpilotni lital'ni aparaty: oznachennya. Klasyfikatsiya, stan ta perspektyvy rozvytku i vykorystannya. Kosmichna nauka i tekhnologiya, 1, 30–43.
[2] Ylyushko V. M., Mytrakhovych M. M., Samkov A. V. , Sylkov V. Y. , Solovev O. V. , Strelnykov V. Y. (2009). Bespilotnye letatel'nye apparaty: Metodiki priblizhennykh raschetov osnovnykh parametrov i kharakteristik. – K.: TsNYY VVT VS Ukrainy.
[3] Zbrutskyy O. V., Masko O. M. , Sukhov V. V. (2012)/ Bezpilotni lital'ni aparaty konteynernogo startu: suchasnyy stan i napryamky doslidzhen'. Visnyk MMI, 64, 63–66.
[4] Kryvokhatko I. S. (2013). Doslidzhennya vplyvu kuta poperechnoho V kryla na aerodynamichni kharakterystyky lital'noho aparatu skhemy «tandem». Mehanika giroskopichnyh system: naukovo-tehnichnyy zbirnyk, 26, 90–101.
[5] Sutuhyn L. Y. (1945). Osnovy proektirovaniya samoletov. – M. : Oborongiz.
[6] Braybrook, R. (2005, June) From scepticism to Sine Quan Non. Retrieved May 09, 2014, from http://www.thefreelibrary.com/From+scepticism+to+Sine+Quan+Non.-a0133864767
[7] Shakhov V. H. (1984). Aerodinamicheskie usovershenstvovaniya i skhemy letatel'nykh apparatov. – Kuybyshev, Kuybyshevskiy aviatsionniy institut im. S. P. Koroleva.
[8] Yur'ev B. N. (1938). Eksperimental'naya aerodinamika. – Chast' 2. Induktivnoe soprotivlenie. – M. : NKOP SSSR.

[9] Kryvokhatko I. S. (2013). Analiz aerodynamiky malogo bezpilotnogo lital'nogo aparatu z teleskopichnym krylom. Voprosy proektirovaniya i proizvodstva konstruktsiy letatel'nykh apparatov. Sborn. nauch. trud. NAU im. Zhukovskogo «KhAI», 3 (75), 107–116.

[10] Vitaliy V. Sukhov, Illia S. Kryvokhatko. (2013). Experimental Investigation Of Aerodynamic Performance Of A Small Uav With A Telescopic Wing . IEEE Ukraine Section Joint SP. AES Chapter. 17–20. DOI: 10.1109/APUAVD.2013.6705272